Diyala Journal of Engineering Sciences

Journal homepage: https://djes.info/index.php/djes

ISSN: 1999-8716 (Print); 2616-6909 (Online)

Performance Enhancement of Shell and Tube Latent Thermal Storage System Using Copper Foam

Luna Sabah*, Jasim Abdulateef

Department of Mechanical Engineering, University of Diyala, 32001 Diyala, Iraq

ARTICLE INFO

Article history:
Received December 6, 2021
Accepted January 4, 2022

Keywords:
Thermal energy storage
PCM
Copper foam
Performance enhancement

ABSTRACT

Latent Heat Thermal Storage (LHTS) based on Phase Change materials (PCMs) offers a promising solution for efficient utilization of intermittent energy from renewable sources. The primary limitation is the poor thermal conductivity of PCMs, which requires employing of thermal performance enhancement techniques. To enhance the thermal performance of PCM thermal energy storage, a copper foam with a high porosity is embedded with the PCM. A numerical simulation model has been developed to investigate the thermal behavior of two LHTS shell and tube configurations: pure PCM-LHTS (conventional LHTS) and PCM - copper-foam composite (foamed LHTS). The effect of the heat transfer fluid (HTF) temperature on the thermal response of LHTS during the charging process was considered. The results showed that the length of melting time for foamed LHTS was shorten about 82% as compared to conventional LHTS under the conditions of HTF temperature of 70°C and flow rate of 0.083 kg/sec. The results show that when the initial temperature of HTF for LHTS with foam was changed from 70°C to 75°C and then from 75°C to 80°C, the total charging time was enhanced by about 33 % and 29%, respectively. Based on results of temperature variation and liquid fraction of PCM, employing copper foam improved the charged thermal load during the charging process compared to LHTS without foam.

1. Introduction

The rise in prices and depletion of fossil fuel associated with increase in greenhouse gas emissions are indicated as the key driving forces behind efforts to successfully utilize several of renewable energy sources. Among the various types of renewable energy resources, solar energy being regarded the best promising energy source in different global parts. Solar energy characteristics like easily and directly utilized being freely available and abundant, continuity and has renewable, and environmentally friendly and safe, making solar energy an interested replacement to the fossil fuels. Furthermore, solar energy suffers from the shortcoming of becoming intermittent with day time, seasons and weather. To overcome the mismatch between energy supply and demand, solar energy systems required thermal energy storage (TES) [1].

Most phase change materials (PCMs) that are used as a storage medium in TES systems, suffering from a low thermal conductivity. This often leads to incomplete melting and solidification processes and also a significant temperature difference within PCM, resulting in material failure and system overheating.

Several studies have been published deal with the employment of porous metal foam to improve the heat transfer exchange and hence, prompting the PCM charging rates.

* Corresponding author.
E-mail address: luna.sabah93@gmail.com
DOI: 10.24237/djes.2022.15304

Zhao et al. [2] studied the heat transfer improvement by introducing metal foam in paraffin using both experimental and computational methods. The effect of metal foam on melting phase transition heat transfer was greater than that of pure PCM, particularly in the solid area of PCM, which may increase the heat transfer rate by 5–20 times. The inclusion of metal foam enhanced the total heat transfer rate by 3–10 times throughout the melting process (two-phase area) and the pure liquid stage. Furthermore, it has been shown that the lower the porosity and pore density, the higher the heat transfer efficiency. **Zhou and Zhao et al. [3]** employed experimentally copper foam with (30 PPI) and expanded graphite (with 3%, 6%, and 9% mass percentage) for enhancement heat transfer of PCMs (paraffin RT 27 and calcium chloride hexahydrate). An increase in thermal conductivity had been detected during melting and solidification which was twice and three times for paraffin and calcium chloride hexahydrate, respectively when metal foam was used. As compared with expanded graphite, the metal foam embedded in PCMs gave better heat storage capacities.

Vadwala et al. [4] investigated experimentally and numerically a method of enhancing the charging and discharging process for TES useing open-cell metal with a high porosity foams. The results showed that the thermal conductivity of composite PCM increased by 16-18 times that of pure paraffin. Also, after the use of metal foam, the time required to melt the PCM was reduced to 36% as compare to TES without foam. It was found that, when the metal foam was used in both wax and air sides, the outlet air temperature increased significantly and the solidification time reduced. **Zhang et al. [5]** investigated numerically the thermal response enhancement LHTS employed with paraffin/graphite foam. Series of numerical calculations were performed to examine the impact of various HTF operating conditions on the charging process of in the system. The findings indicated that thermal performance can be enhanced effectively with graphite foam additive.

Li and Wu. et al [6] simulated numerically the thermal behavior of sodium nitrate (NaNO3) as a phase change material with the porous metal matrix. The results clarified that the melting and solidification times had decreased by up to 20% and 3.9%, respectively of that with pure PCM and for 90% porosity. Further, it is found that the porosity was effective in improving heat transfer in which pore density did no effect.

Jialin Yang et al. [7] studied experimentally the addition of metal foam and bottom fin to PCM to improve the thermal behaviour of shell and tube TES. When the copper foam and bottom fin added to the PCM, the completed melting time of foamed LHTS takes about 1/3 shorter time than pure paraffin at the same temperature conditions, according to the experiments. The composite with a bottom fin had the shortest overall charging time and the highest heat transfer rate.

Tao et al. [8] used Lattice Boltzmann approach to evaluate the TES performance of metal foams/paraffin composite PCM. The impact of metal foam porosity and PPI on PCM melting rate, heat storage capacity, and heat storage density was examined. The results show that the proposed scheme can improve the uniformity of the heat transfer process and enhance the heat transfer performance.**Jialin et al. [9]** investigated a thermal behavior of a shell-and-tube LHTS. The paraffin wax was mixed with copper foam. The findings showed that under the same operating conditions, it takes approximately 1/3 less time to completely melt PCM in composite than pure paraffin. The composite PCM consumes the least amount of overall charging time and has the highest heat transfer rate. The temperature of the HTF has a significant impact on the charging process than the flow rate of the HTF. **Zhang et al. [10]** examined the melting heat transfer properties of the paraffin-copper foam composite PCM experimentally and statistically. In comparison to pure paraffin, composite PCM demonstrated superior heat transfer. **Mehdi et al. [11]** used an enhancement technique of a compound porous-foam/nanoparticles in a triplex tube heat exchanger (TTHX) applicable to liquid desiccant air-conditioning applications. Results showed that dispersing nanoparticles in the presence of metal foams results in total time

saving up to 96% depending on foam structure and volumetric nanoparticle concentration.

Matthieu et al. [12] used an enhancement technique of a copper foam-PCM composite in shell-and-tube LHTS. The effect of either upward and downward flows have been investigated on melting and solidification. The results showed that, the charging/discharging time consumption of the foamed tube is faster ten times than a bare tube. **Hiba et al [13]** investigated experimentally the improvement of performance of Cascaded Thermal Energy Storage (CTES) using metal foam-PCM composite during discharging. The results obtained indicated that a decrease in the solidification time consumption can be achieved with inclusion of metal foam. In addition, they found that smaller foam porosity shows better discharging performance. **Wang et al. [14]** studied the charging/discharging properties of copper foams using a vertical shell-and-tube LHTS tube with radial gradient porosity. They claimed that as compared to the homogenous copper foam, the total melting time was reduced by 37.6 %. **Mahdi et al. [15]** studied on the multiple PCMs distribution in a double-tube LHTS unit during the solidification including nanoparticles and metal foam. The results showed 94% improvement in the solidification time for the best scenario.

The aim of this study is to improve the thermal performance of shell and tube LHTS by inclusion a high conductivity porous material. Since copper has the highest heat conductivity at among the metals, the open cell copper foam-PCM composite was used in the LHTS during the charging process. The thermal performance of LHTS was investigated in terms of PCM temperature evolution, charging time, and PCM liquid fraction, at various input HTF temperature and constant flow rate.

2. Numerical Model

A numerical simulation for the problem of the present work was developed to investigate the melting process of PCM with and without the addition of metal foam in LHTS. For this purpose, two different simulation models were developed with the help of CFD tool using ANSYS Fluent19.

The enthalpy-porosity technique is used to simulate the melting process of PCM [16,17,3]. This approach produces more precise simulation results and a more realistic depiction of the underlying processes. Additionally, there is no explicit monitoring of the solid-liquid interface; instead, it is determined by the liquid fraction (β), which reflects the percentage of liquid in a particular cell in the modeling domain.

The value of the liquid fraction, (β), is then [18];

$$\begin{aligned} &\beta = 0 && \text{for } T < T_{solidus} \\ &\beta = \frac{T - T_{solidus}}{T_{liquidus} - T_{solidus}} && \text{for } T_{liquidus} < T < T_{solidus} \\ &\beta = 1 && \text{for } T > T_{liquidus} \end{aligned} \quad (1)$$

where T is the local temperature.

Therefore, the following variables influence the velocity;

$$\begin{aligned} &V = V_1 && \text{in the liquid phase} \\ &V = \beta V_1 && \text{in the mushy zone} \\ &V = 0 && \text{in the solid phase} \end{aligned} \quad (2)$$

where V is the superficial velocity (i.e., the ensemble-average velocity), and V_1 is the actual velocity [16].

The gravitational acceleration is along the y-axis and the Boussinesq approximation is considered so as to take into account the buoyancy force due to natural convection, thus the density of PCM varies with temperature [19];

$$\rho = \rho_0 [1 - \gamma(T - T_0)] \quad (3)$$

where ρ is the PCM local density, T_0 and ρ_0 are the operating temperature and density, and γ is the thermal expansion coefficient. The metal foam is modelled as an isotropic homogeneous with a Darcy-Forchheimer law (modified Darcy law for high-speed flow) because it behaves like a porous medium, and the flow of the liquid PCM in metal foam is assumed Newtonian, incompressible, with laminar flow [20].

The governing equations of continuity, momentum and thermal energy for the model can be summarized as follows [19,21,22]:

Continuity Equation

$$\frac{\partial \rho}{\partial t} + \nabla.(\rho \overrightarrow{V}) = 0 \quad (4)$$

where t is the time.

Momentum Equations

$$\rho\left(\frac{\partial \overrightarrow{V}}{\partial t} + (\nabla.\overrightarrow{V})\overrightarrow{V}\right) = \mu(\nabla^2\overrightarrow{V}) - \nabla P + \vec{s} \quad (5)$$

where μ is the viscosity of the PCM, P is the pressure, the vector $\vec{s}$ is a global source term given by the following form:

$$\vec{s} = \frac{(1-\beta)^2}{(\beta^3+€)^3} Amush\ \overrightarrow{V} + \rho\vec{g}\gamma(T - T_0) + \frac{\mu}{\alpha}\overrightarrow{V} + \frac{C_F}{\sqrt{\alpha}}\rho\overrightarrow{V}\left|\vec{V}\right| \quad (6)$$

The first term after equal sign due to the presence of the solid PCM in the mixed region, where € is small number (less than 0.001) to prevent division by zero [23]. $Amush$ is the mushy zone constant which acts as a damping factor of the velocity during PCM solidification. In literatures its value is usually varied from 10^4 to 10^7 , but [24] performs a simulation for a range of its values and found that 10^5 gave the best results. Hence, its value is set to 10^5 kg/m³s in the simulation cases of the present research study. The second term is the Boussinesq approximation, which is necessary for modeling natural convection in PCM liquid phase. The vector $\vec{g}$ is the gravitational acceleration which equal to (0 m/s²) in the x- and z-directions and equal to (-9.81 m/s²) in the y-direction. The third term is the Darcy term and the last term is the Forchheimer (or inertia) term, metal foam resistances to the flow of PCM, where a and $C_F$are the permeability and the inertial drag factor respectively, of the metal foam. They are calculated by the following [25];

$$\alpha = 0.00073(1-\varepsilon)^{-0.224}\left(\frac{d_f}{dp}\right)^{-1.11}(d_p)^2 \quad (7)$$

$$C_F = 0.000212(1-\varepsilon)^{-0.132}\left(\frac{d_f}{dp}\right)^{-0.163} \quad (8)$$

where d_f, dp and are the ligament diameter, the pore diameter and the porosity of the metal foam respectively. They are linked to the other metal foam parameters by the following equations 25.

$$\frac{d_f}{dp} = 1.18\sqrt{\frac{1-\varepsilon}{3\pi}}\left(\frac{1}{\frac{1-e^{-(1-\varepsilon)}}{0.04}}\right) \quad (9)$$

$$dp = \frac{0.0224}{\omega} \quad (10)$$

where ω is the port density.

Energy Equation

$$\frac{\partial}{\partial t}(\rho h) + \nabla.(\rho\overrightarrow{V}h) = k_{eff}\nabla^2 T - \varepsilon\rho L\frac{\partial \beta}{\partial t} \quad (11)$$

where L is the latent heat of the PCM, h is the sensible enthalpy can be described as [26,105];

$$h = h_{ref} + \int_{T_{ref}}^{T} C\ dT + \beta L \quad (12)$$

where h_{ref} is the reference temperature enthalpy T_{ref}, and C is the specific heat of liquid. The effective thermal conductivity k_{eff} in equation (11) is calculated as the volume average of the conductivities of porous material and PCM, which are denoted by;

$$k_{eff} = (1-\varepsilon)k_{m.f.} + \varepsilon k_{PCM} \quad (13)$$

where $k_{m.f.}$and k_{PCM} are the thermal conductivities of metal foam and PCM, respectively.

During the charging process, heat flows from the high temperature HTF to low temperature PCM and the opposite occurs during the discharge process. The water is used as HTF, which can be considered as incompressible and Newtonian fluid, and the flow is turbulent. The (k- ε) standard turbulence model was applied to the turbulence of flow [28,29].

Three-dimensional models are utilized to simulate the instances in this research, which are divided into four stages: geometry creation, meshing, post-processing, and eventually analysis. In the present study, the SOLID WORK (version18) program was used to create the geometric models, including specifying the HTF and PCMs zones.

Different grid densities were evaluated to achieve grid independence for a three-dimensional model with a different number of elements for the water and PCM zone [1450982, 815080, 356290 and 200884]. The numerical results have shown that the total number of elements 356290 is appropriate as it reflects the optimal trade-off between solution precision

and reliability and the computational cost. The cell type was Hex/wedge element and the type is cooper cell for a three-dimensional. After reaching a successful mesh, the models were exported to fluent for setup and analysis processes. A time step value of 0.1s was chosen to save computing capacity. The melting model is enabled for the PCM melting process, with the mushy zone constant set at 10^5.

The selected materials for these simulations are:

- Paraffin is used as PCMs.
- Water was used as HTF various from (343.14k) to (353.14k).
- Copper was used as a material of metal foam and the surface of separation between PCMs and HTF.
- Perspex was used as an insulator between adjacent PCMs and for perimeter walls.

The thermophysical properties of these materials are listed in Table 1.

Table 1: Thermo-Physical Properties used in LHTS Simulation.

Material / Properties	PCM (Paraffin wax)	Water	Copper
Melting temperature range (C°)	48-62	-	-
Latent heat (J/kg. C°)	114540	-	-
Specific heat (J/kg. C°)	2000(liquid)	4190	385
Density (kg/m³)	820 (liquid at 65 C°)	996	873.03
Thermal conductivity (W/m. K)	0.14 (solid at 30 C°)	0.66	387.6
Viscosity (Pa.s)	0.033 (at 65 C°)	0.001	-
Thermal expansion coefficient (1/K)	6×10^{-4}	-	-

The HTF copper tube has an outside diameter of 1.92 cm and a thickness of 0.1 cm. Water flows through the 19.2mm outer diameter copper tube located centrally in the external cylindrical tube, which is assumed made of transparent Plexiglass with dimension of 460 mm in length and 70 mm in inner diameter. The copper foam of open cell type was used in the present study and has a porosity of 0.9 and a port density of 10 PPI (pores per inch). The shell and tube thermal storage used in numerical simulation is shown in Fig.1.

A mass flow rate inlet boundary condition type was selected for HTF at both entrances, see Fig. 1. The boundary condition type was set as pressure outlet type for HTF at both exits. Other walls were considered completely insulated, indicating that they were in an adiabatic thermal state. Except for the walls between the PCMs and the HTF, it was subjected to coupled temperature conditions to facilitate heat exchange.

For the velocity-pressure coupling, the SIMPLEC (Semi-Implicit Method for Pressure Linked Equations-Consistent) method was used. To improve the convergence's stability, we evaluated under-relaxation values of 0.7, 0.3, 1, 0.9, and 1 for momentum, liquid fraction, pressure, turbulent viscosity, and energy respectively. The CFD simulation is carried out by using a high-performance PC with (Core i7 CPU 9750H with 2.60 GHz, RAM: 16 GB, and System type MSI Raider 95 E 9^{th} generation). The computing time of the shell and tube LHTS was about (10-15 days).

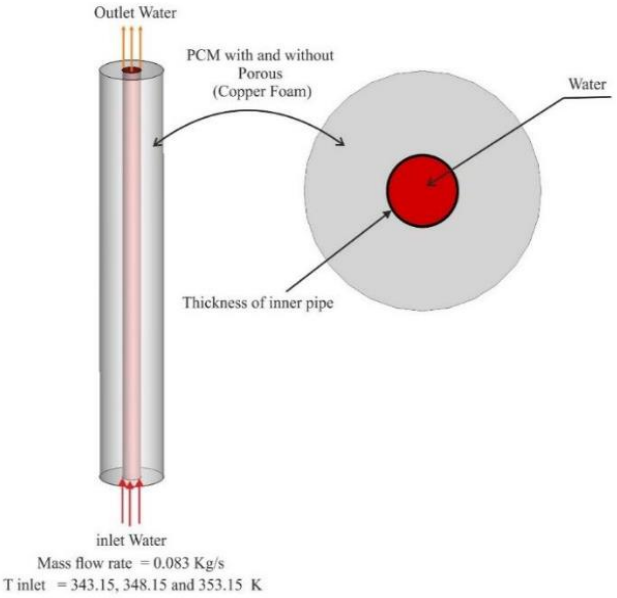

Figure 1. Shell and tube LHTS used in CFD simulation

3. Results and discussion

The numerical results obtained from numerical simulation for Both a pure PCM tube (LHTS without foam) and a PCM-copper foam tube (foamed LHTS) were discussed in terms of PCM temperature variation, melting time and liquid fraction contours.

A comparison for the numerical simulation between the present study and available literature was performed with respect to liquid fraction during the charging process. The comparison is presented for a pure PCM LHTS configuration that was arranged vertically.

Figure 2 shows that a qualitative comparison of the melting front for present numerical results with previous observation [30] at the same flow and design parameters, which clearly demonstrates that the melting front is moving downward at about the same rate in both cases.

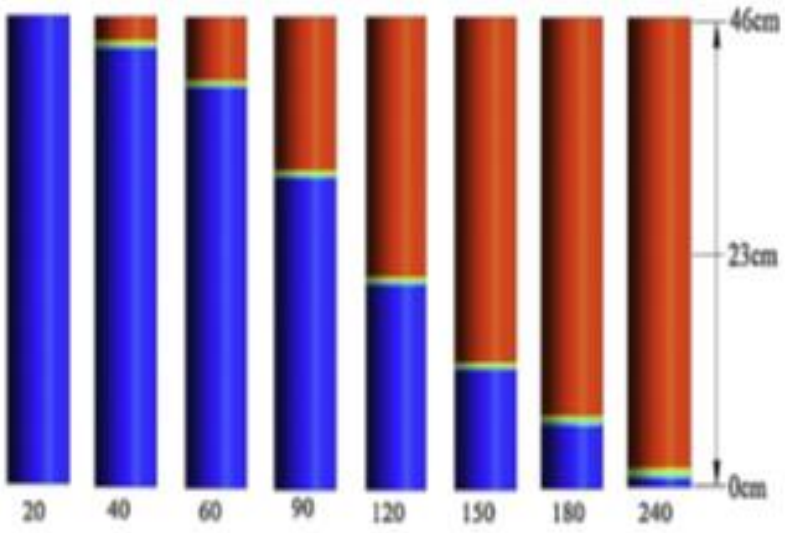

(a)

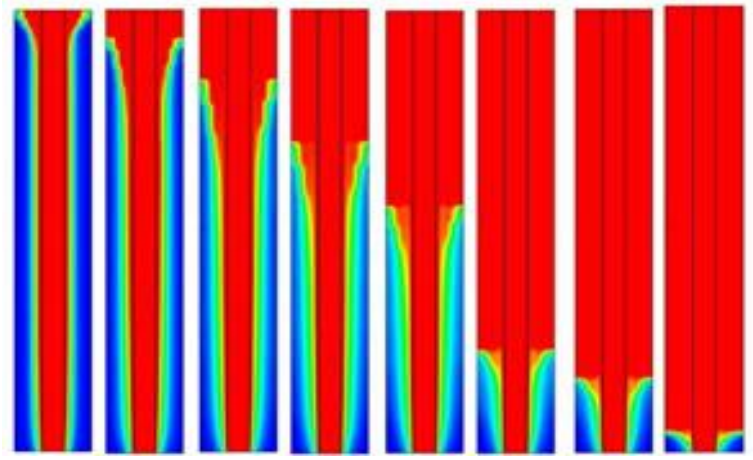

(b)

Figure 2. Evolution of liquid fraction d contours in vertical pure PCM shell and tube LHTS (T_{HTF}= 73 ºC, vertical $\dot{m}$= 5 l/m): (a) previous study [30], (b) present study

Figure 3 shows the evolution of PCM average temperature for both LHTS configuration arranged vertically at THTF=75oC, 5 l/min flow rate.

Clearly, the overall fluctuation in PCM temperature may be classified into three different periods. Period begins when the melting process started (i.e. T=30 °C) and concludes when the PCM begins to melt (i.e. T=48 °C). Almost completely throughout this time period, heat is transferred from the heated HTF to the solid PCM by conduction. Period II begins when the temperature exceeds 48 °C. Due to the passage of the melting front, the PCM temperature rises rapidly during this time. This period is determined by the temperature range of the PCM melting point (48 - 62°C). Period III is initiated in this instance at a temperature range of 62–73°C.

As shown in Fig. 3, the average temperature of PCM for foamed LHTS changes dramatically as the PCM melts. As time passes, the rate of increase in the average temperature of PCM is much faster in foamed LHTS than in sample LHTS. The total time required by LHTS to melt PCM is 370 minutes for a basic LHTS configuration and 65 minutes for a foamed LHTS configuration, respectively. The saving in melting time was about 82 % in melting time. As explained before, the employing of high thermal conductivity material with PCM transfers large amount of heat into the internal part easily and thus significantly shorten the melting process.

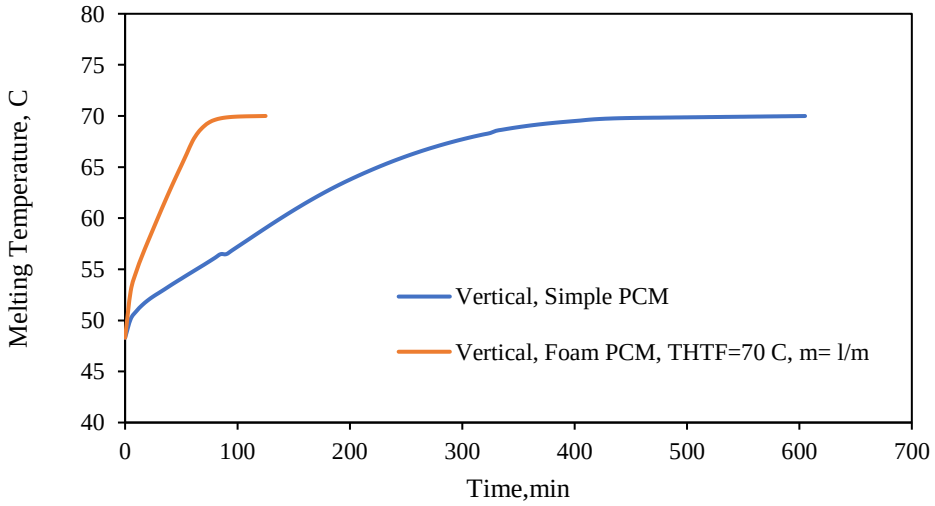

Figure 3. Transient variation of average temperature of PCM during melting of LHTS (T_{HTF}=70 oC, m= 5 l/m)

The development of the solid–liquid interface for the pure PCM tube at THTF=70 ºC and (m_{HTF})=5 l/m is shown in Fig. 4. Within about 25 minutes, the PCM mass near the tube wall melted, and the solid–liquid interface assumed the form of a cylindrical surface parallel to the tube's axis.

By buoyancy, the molten paraffin absorbs heat from the HTF and flows higher toward the heating tube. The molten PCM direction flow changes at the upper boundary, and it flows down along the solid–liquid interface, releasing heat to the melting front.

The development of the PCM contours demonstrates that the top portion overheats while the lower portion does not melt. It is caused by PCM low conductivity, natural convection flow, and the shell-and-tube construction of the LHTS unit. Additionally, the density of molten PCM is less than the density of solid phase. As a result, the area of molten PCM gradually expands to include the majority of the upper PCM LHTS container.

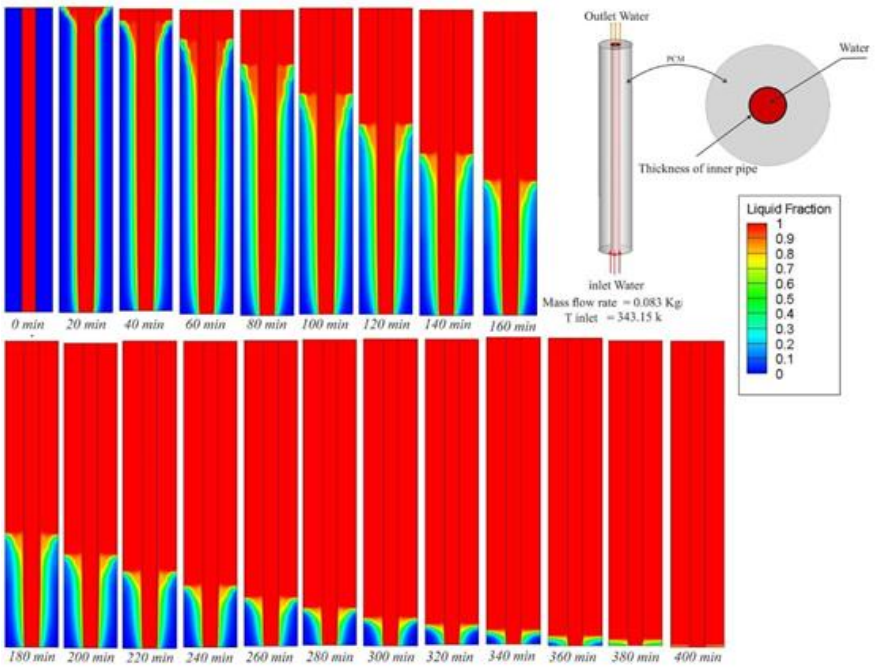

Figure 4. Liquid fraction contours of LHTS without foam during melting process (T_{HTF}= 70 ºC, $\dot{m}$= 5 l/m,)

Under the condition of the same HTF flow rate and heating temperature and same weight of PCM, the numerical results for foamed tube are obtained. Figure. 5 shows the evolution of solid–liquid interface for foamed LHTS in vertical position.

In contrast to the pure PCM condition, where the solid–liquid interface develops and observed clear gradually after 60 minutes, the solid–liquid interface forms and becomes clear gradually after 20 minutes. This is because foam thermal storage has a higher effective thermal conductivity, which allows heat to be rapidly transmitted into the internal part of the shell.

Copper foam significantly improves heat transfer and the phenomena where the bottom portion does not melt as rapidly as the upper part. The reduction in charging time is significant as a result of the use of copper foam. In comparison to pure PCM tubes, the overall melting time is decreased by 82 %.

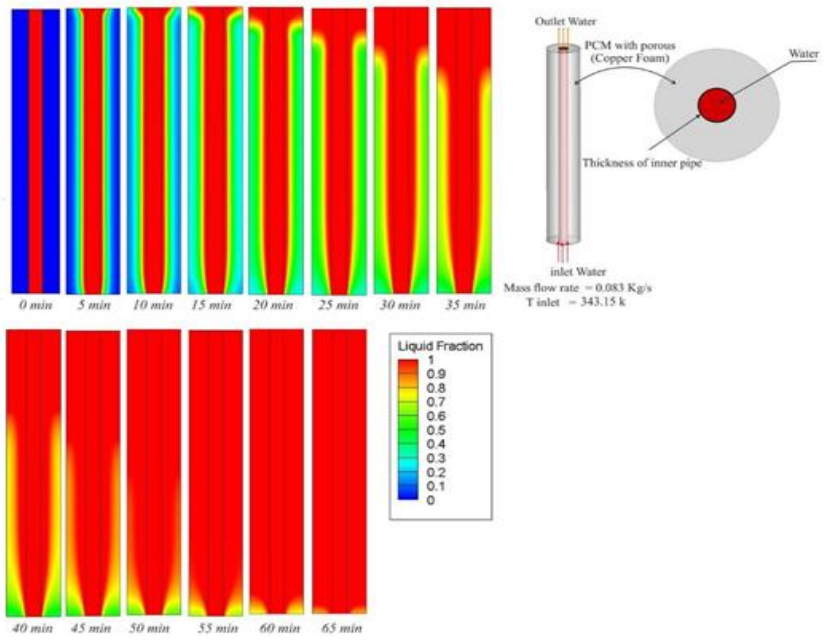

Figure 5. Liquid fraction contours of LHTS with foam during melting process (T_{HTF}= 70 ºC, $\dot{m}$= 5 l/m)

The impact of the HTF temperature on the PCM average temperature during the charging process for foamed LHTS configuration in vertical position is shown in Fig. 6. The overall conclusion is that the HTF's inlet temperature has a considerable effect on the rate of PCM melting. Obviously, increasing the initial temperature of HTF leads in a considerable decrease in the overall PCM melting time. When the initial temperature of HTF was changed from 70°C to 75°C and then from 75°C to 80°C, the total melting time was reduced about 33% and 29%, respectively.

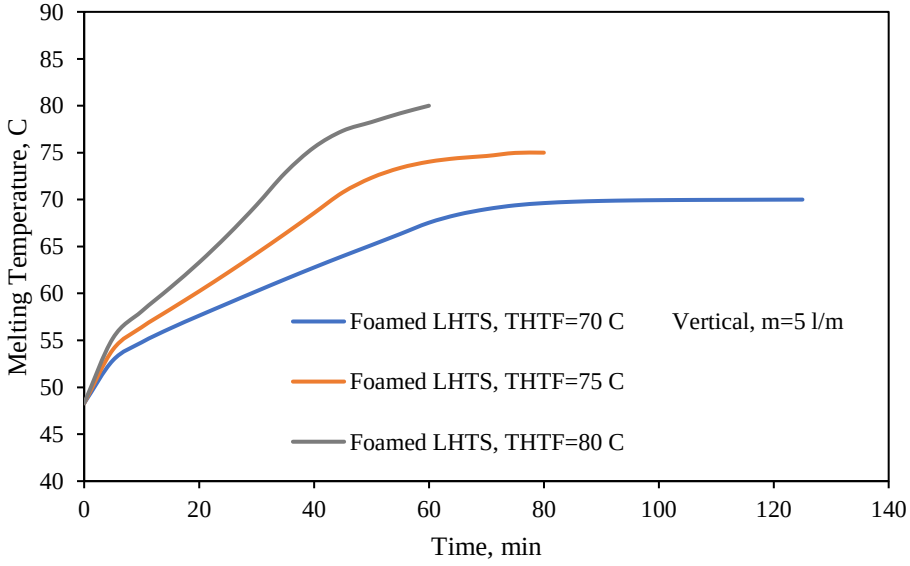

Figure 6. Effect of HTF temperature on total charging time of LHTS with foam

4. Conclusions

The thermal performance of LHTS are evaluated numerically in terms of the transient temperature distribution of PCM, the time required to charge, the liquid fraction of PCM, during melting process at different inlet temperatures and constant mass flow rates of

HTF. The influence of varying the inlet HTF temperature on the LHTS performance is investigated at three different temperatures: 70 ℃, 75 ℃, and 80 ℃. The mass flow rate 0.083 kg/sec is of HTF through the LHTS which is maintained at a constant level continuously.

The following conclusions can be drawn:

- A rapid completed melting at the upper portion in LHTS arranged vertically can be distinguished for latent heat thermal storage with and without foam samples at vertical orientation.
- The inclusion of high thermal conductivity material with PCM transfers large amount of heat into the internal part of shell and tube thermal storage easily and thus significantly shorten the melting process.
- The time required for completed charging of foamed LHTS configuration was reduced about 82% compared to LHTS without foam under the conditions of HTF temperature of 70°C and flow rate of 0.083 kg/sec.
- Significant effect for HTF variation on heat transfer characteristics of LHTS system with copper foam. The saving time in charging time was found about 33% and 29% when HTF temperature changed from 70 ^{o}C to 75oC and 75^{o}C to 80^{o}C respectively.

References

[1] Surbu I. and Dorca A., “Review on heat transfer analysis in thermal energy storage using latent heat storage systems and phase change materials” Wiley International journal of energy research, (2018).

[2] Zhao, C. Y., W. Lu, and Yuan Tian. "Heat transfer enhancement for thermal energy storage using metal foams embedded within phase change materials (PCMs)." Solar energy 84.8 (2010): 1402-1412.

[3] Zhou, Dan, and C. Y. Zhao. "Experimental investigations on heat transfer in phase change materials (PCMs) embedded in porous materials." Applied Thermal Engineering 31.5 (2011): 970-977.

[4] Vadwala, H. "Thermal energy storage in copper foams filled with paraffin wax." Doktori disszertáció, Mechanical & Industrial Engineering University of Toronto (2012).

[5] Guo, C. X., W. J. Zhang, and D. B. Wang. "Numerical investigations of heat transfer enhancement in a latent heat storage exchanger with paraffin/graphite foam." International Conference on Heat Transfer, Fluid Mechanics and Thermodynamics, 2014.

[6] Li, Zhuo, and Zhi-Gen Wu. "Numerical study on the thermal behavior of phase change materials (PCMs) embedded in porous metal matrix." Solar Energy 99 (2014): 172-184.

[7] Yang, Jialin, et al. "Experimental study on enhancement of thermal energy storage with phase-change material." Applied Energy 169 (2016): 164-176.

[8] Tao, Y. B., Y. You, and Y. L. He. "Lattice Boltzmann simulation on phase change heat transfer in metal foams/paraffin composite phase change material." Applied Thermal Engineering 93 (2016): 476-485.

[9] Yang, Jialin, et al. "Experimental study on enhancement of thermal energy storage with phase-change material." Applied Energy 169 (2016): 164-176.

[10] Zhang, Feng, et al. "Encapsulation of metal-based phase change materials using ceramic shells prepared by spouted bed CVD method." Solar Energy Materials and Solar Cells 170 (2017): 137-142.

[11] Mahdi, Jasim M., and Emmanuel C. Nsofor. "Solidification enhancement in a triplex-tube latent heat energy storage system using nanoparticles-metal foam combination." Energy 126 (2017): 501-512.

[12] Martinelli, Matthieu, et al. "Experimental study of a phase change thermal energy storage with copper foam." Applied thermal engineering 101 (2016): 247-261.

[13] Hasan, Hiba Abdulameer. Thermal Performance Enhancement of Phase Change Materials (PCMs) by Using Cascade Thermal Energy Storage (CTES) System with Metal Foam. Diss. University of Baghdad, 2018.

[14] Wang, Zhifeng, et al. "Experimental study on latent thermal energy storage system with gradient porosity copper foam for mid-temperature solar energy application." Applied Energy 261 (2020): 114472.

[15] Mahdi, Jasim M., et al. "Solidification enhancement with multiple PCMs, cascaded metal foam and nanoparticles in the shell-and-tube energy storage system." Applied Energy 257 (2020): 113993.

[16] Voller, Vaughan R., and C. Prakash. "A fixed grid numerical modelling methodology for convection-diffusion mushy region phase-change problems." *International journal of heat and mass transfer* 30.8 (1987): 1709-1719.

[17] Al-abidi A., Mat S.B., Sopian K., Sulaiman M.Y., Mohammed A.Th., "CFD application for latent heat thermal energy storage: a review", Renewable and Sustainable Energy Review, Vol. 20, pp. 353-363, (2013).

[18] Hesaraki, Arefeh. *CFD modeling of heat charging process in a direct-contact container for mobilized thermal energy storage*. 2011.

[19] Buonomo, Bernardo, et al. "Numerical simulation of thermal energy storage with phase change material and aluminum foam." (2016).

[20] Zhang, Peng, et al. "Experimental and numerical study of heat transfer characteristics of a paraffin/metal foam composite PCM." *Energy Procedia* 75 (2015): 3091-3097.

[21] Saraswat, Amit, et al. "Latent Heat Thermal Energy Storage in A Heated Semi-Cylindrical Cavity: Experimental Results and Numerical Validation." *changes* 5 (2015): 7.

[22] Liu, Zhenyu, Yuanpeng Yao, and Huiying Wu. "Numerical modeling for solid–liquid phase change phenomena in porous media: Shell-and-tube type latent heat thermal energy storage." *Applied energy* 112 (2013): 1222-1232.

[23] Nithyanandam, K., and R. Pitchumani. "Computational studies on metal foam and heat pipe enhanced latent thermal energy storage." *Journal of heat transfer* 136.5 (2014).

[24] Soibam, Jerol. *Numerical Investigation of a Phase Change Materials (PCM) heat exchanger-For small scale combustion appliances*. MS thesis. NTNU, 2017.

[25] Calmidi, Varaprasad V., and Roop L. Mahajan. "Forced convection in high porosity metal foams." *J. Heat Transfer* 122.3 (2000): 557-565.

[26] Korawan, Agus Dwi, et al. "3D numerical and experimental study on paraffin wax melting in thermal storage for the nozzle-and-shell, tube-and-shell, and reducer-and-shell models." *Modelling and Simulation in Engineering*, 2017.

[27] Guo, C. X., W. J. Zhang, and D. B. Wang. "Numerical investigations of heat transfer enhancement in a latent heat storage exchanger with paraffin/graphite foam." International Conference on Heat Transfer, Fluid Mechanics and Thermodynamics, 2014.

[28] Sciacovelli A., Colella F., and Verda V., "Melting of PCF in thermal energy storage unit: Numerical investigation and effect of nanoparticle enhancement", International Journal of Energy Research (2012).

[29] Hammendy B. M. H. "Experimental and Numerical Model of a Phase Change Material (PCM) with Thermal Conductivity Enhancers", M.SC. Thesis, Al-Mustansiriyah University, (2015).

[30] Mahdi, Mustafa S., et al. "Numerical study and experimental validation of the effects of orientation and configuration on melting in a latent heat thermal storage unit." Journal of Energy Storage 23 (2019): 456-468.